Molecular Dynamics, Free Energy, and SPR Analyses of the Interactions between the SH2 Domain of Grb2 and ErbB Phosphotyrosyl Peptides

Atsushi Suenaga,*,‡,§ Mariko Hatakeyama,‡,§ Mio Ichikawa,‡ Xiaomei Yu,‡ Noriyuki Futatsugi,‡ Tetsu Narumi,‡ Kazuhiko Fukui,|| Takaho Terada,⊥ Makoto Taiji,‡ Mikako Shirouzu,⊥ Shigeyuki Yokoyama,⊥,#,▽ and Akihiko Konagaya‡

Bioinformatics Group, RIKEN Genomic Sciences Center, 1-7-22 Suehiro-cho, Tsurumi-ku, Yokohama, Kanagawa 230-0045 Japan, Protein Research Group, RIKEN Genomic Sciences Center, 1-7-22 Suehiro-cho, Tsurumi-ku, Yokohama, Kanagawa 230-0045 Japan, Computational Biology Research Center (CBRC), National Institute of Advanced Industrial Science and Technology, 2-41-6 Aomi, Koutou-ku, Tokyo 135-0184 Japan, Cellular Signaling Laboratory/Structurome Research Group, RIKEN Harima Institute at SPring-8, 1-1-1 Kohto, Mikazuki-cho, Sayo, Hyogo 679-5148 Japan, and the Department of Biophysics and Biochemistry, Graduate School of Science, The University of Tokyo, 7-3-1 Hongo, Bunkyo-ku, Tokyo 113-0033 Japan

Received January 21, 2003; Revised Manuscript Received February 27, 2003

ABSTRACT: We studied the interactions between the SH2 domain of growth factor receptor binding protein 2 (Grb2) and ErbB receptor-derived phosphotyrosyl peptides using molecular dynamics, free energy calculations, and surface plasmon resonance (SPR) analysis. Binding free energies for nine phosphotyrosyl peptides were calculated using the MM-PBSA continuum solvent method, and excellent qualitative agreement with the SPR experimental data, with a correlation coefficient of 0.92, was obtained. Consistent with previous experimental findings, phosphotyrosyl peptides with the consensus sequence pYXNX showed favorable binding affinity for the Grb2. Unexpectedly, phosphotyrosyl peptides with the consensus sequence pYQQD, which had not shown any specific binding affinity for the Grb2 in earlier studies, also showed favorable binding affinity for the Grb2 in our experimental and computational analyses. Component analysis of the calculated binding free energies revealed that van der Waals interaction between the Grb2 and the phosphotyrosyl peptide was the dominant factor for specificity and binding affinity. These results indicate that current methods of estimating binding free energies are efficient for obtaining important information about protein−protein interactions, which are essential for the transmission of signals in cellular signaling pathways.

As the regulatory mechanisms of adaptor proteins in signal transduction cascades are revealed, adaptor proteins are readily gaining importance as new drug targets (*1*). The growth factor receptor binding protein 2 (Grb2)[1] is composed of one Src homology 2 (SH2) domain and two SH3 domains. It links several membrane receptor kinases and the SH3 binding molecules, thereby activating the Ras-MAPK cascade (*2*, *3*). The SH2 domain of Grb2 binds to phosphotyrosyl residues on various membrane receptors, such as IGF-I receptors (*4*), TrkA receptors (*5*), ErbB receptors (*6*), and platelet-derived growth factor (PDGF) receptors (*7*), and to adaptor proteins such as FRS and Shc (*5*).

Surface plasmon resonance (SPR) and isothermal titration calorimetry (ITC) are two popular biochemical techniques for measuring direct protein−protein/peptide interactions and produce virtually identical results (*8*). Analysis of interactions between phosphotyrosyl peptides (P-peptides) and the Grb2 protein and Grb2 SH2 domain have been conducted independently by many research groups, and pYXNX was determined to be a Grb2 binding peptide (*9*−*11*). However, a recent study has suggested that the pYXNX sequence is a highly cross-reactive SH2 binding site and not a Grb2 specific binding motif (*12*). This study showed that N at $p + 2$ functions as the main determinant for Grb2 SH2 affinity and that the residue on $p + 1$ serves as a prime determinant for Grb2 SH2 specificity; it concluded that the pYKNI/L sequence is specific for Grb2 SH2 binding. In the realm of cell biology, however, it is difficult to apply this strategy to distinguish the specific binding sites for Grb2 in ErbB receptors. For example, pY1068 (pYINQ) and pY1086 (pYHNQ) in ErbB1 (=EGF receptor) are specific binding regions for the Grb2 SH2 domain (*9*−*11*); however, ErbB4 pY1188 (pYHNA) and pY1242 (pYWNH) have been determined to be Shc binding sites (*13*).

Molecular dynamics (MD) simulation has been useful in investigating protein−protein, protein−ligand, and protein−

* To whom correspondence should be addressed. Tel.: +81-45-825-7868. Fax: +81-45-825-7854. E-mail: suenaga@gsc.riken.go.jp.
§ These authors contributed equally to this research.
‡ Bioinformatics Group, RIKEN Genomic Sciences Center.
|| National Institute of Advanced Industrial Science and Technology.
⊥ Protein Research Group, RIKEN Genomic Sciences Center.
Cellular Signaling Laboratory/Structurome Research Group, RIKEN Harima Institute at SPring-8.
▽ The University of Tokyo.

[1] Abbreviations: Grb2, growth factor receptor binding protein 2; GST, glutathione *S*-transferase; MAPK, mitogen-activated protein kinase; MD, molecular dynamics; MDM, molecular dynamics machine; MM-PBSA, molecular mechanics Poisson−Boltzmann surface area; SH2, Src homology 2 domain; Shc, Src homology and collagen domain protein; SPR, surface plasmon resonance.

10.1021/bi034113h CCC: $25.00
Published on Web 04/12/2003

DNA interactions at the atomic level. A new method, molecular mechanics Poisson−Boltzmann surface area (MM-PBSA), was recently proposed for calculating the binding free energies of macromolecules (*14*, *15*). This method combines MD simulations in explicit solvent with implicit solvation models, Poisson−Boltzmann (PB) analysis (*16*−*19*), and solvent accessible surface area (*20*) to estimate free energies. The free energy of the macromolecular system consists of contributions from van der Waals and electrostatic energies, nonpolar and electrostatic solvation energies, and relative solute entropy effects (*21*). The van der Waals and electrostatic energies are calculated using molecular mechanics (MM); the nonpolar solvation energy is estimated using empirical methods based on the solvent accessible surface (SA); and the electrostatic solvation energy is obtained by using a continuum solvation model and solving the PB equation. The entropy contribution can be estimated using normal-mode analysis (*22*). In previous studies, the MM-PBSA method has been successfully applied in the calculation of binding free energies (*23*−*27*).

A special purpose computer for MD, the Molecular Dynamics Machine (MDM), can calculate large-scale long-range interactions (van der Waals and Coulomb) with high speed and accuracy (*28*). The MDM allows us to perform several MD simulations for estimating binding free energies between a receptor protein and its various ligands on a realistic time scale.

In this study, we used the MDM for MD simulations of the Grb2 complexed with the nine different P-peptides to estimate their binding free energies, and these binding free energies were compared with SPR experimental data. We conducted SPR analysis of the kinetic constants and affinities for the binding of full-length Grb2 protein and Grb2 SH2 domain with nine P-peptides derived from ErbB1 and ErbB4. Our results were further confirmed by the free energy change (ΔG) produced by the interaction of the Grb2 SH2 domain and P-peptides using MD simulations and the MM-PBSA method. Computational analyses reproduced the ligand specificity for all the ErbB P-peptides tested in our SPR experiments, which means that MD simulation can be used for in silico screening for Grb2-binding ligands. The MDM is a very effective tool for such analysis.

MATERIALS AND METHODS

P-Peptide Synthesis. P-peptides in which the N-terminal was biotinylated were synthesized by a PMSS8 synthesizer (Shimazu, Inc.) with the *N*α-*N*-(9-fluorenyl) methoxycarbonyl (Fmoc) method using 2-(1H-benzotriazole-1-yl)-1,1,3,3-tetramethyluronium hexafluorophosphate (HBTU) (Toray Research Center, Inc.). The sequences corresponding to human ErbB-derived P-peptides are listed in Table 1.

Protein Expression and Purification. cDNA encoding full-length human Grb2 (a.a. 1−217) and Grb2 SH2 domain (a.a. 60−152) were subcloned in the expression vector pGEX (Amersham Biosciences), and glutathione *S*-transferase (GST) fusion proteins were produced in *Escherichia coli* through isopropyl β-D-thiogalactopyranoside induction; the proteins were then purified with GSTrap column (Amersham Biosciences) according to the manufacturer's protocol. The Grb2 SH2 domain was dialyzed against HEPES buffer [20 mM HEPES (pH 7.0), 2 mM dithiothreitol (DTT)]. The full-length Grb2 GST fusion proteins were further subjected to anion exchange chromatography in 20 mM Tris-HCl (pH 8.0), 1 mM DTT and eluted with gradient elution of 1 M NaCl. The GST fusion proteins obtained were pooled and dialyzed with 20 mM HEPES (pH 7.0), 2 mM DTT. The purities of the samples were checked using SDS−PAGE, and the protein concentrations were determined with Protein Assay Reagent (Bio-Rad).

Table 1: Amino Acid Sequences of P-Peptides

P-peptide	sequence[a]
ErbB1 pY0992	DDVVDADE*pY*LIPQQGFFFS
pY1045	KEDSFLQR*pY*SSDPTGA
pY1068	DTFLPVPE*pY*INQSVPKR
pY1086	AGSVQNPV*pY*HNQPLNPAPS
pY1148	QISLDNPD*pY*QQDFFPKEAK
pY1173	GSTAENAE*pY*LRVAPQSSE
ErbB4 pY1056	HSPPPA*pY*TPMSGNQ
pY1188	KNGDLQALDNPE*pY*HNASNGP
pY1242	PEKAKKAFDNPD*pY*WNHSLPP

[a] *pY* is phosphotyrosine.

Interaction Analysis. BIAcore 3000 system (Pharmacia, Inc.) was used to experimentally determine the kinetic constants of the protein−P-peptides interactions. Sensor chip SA was preconditioned with a solution containing 1 M NaCl and 50 mM NaOH, and biotinylated P-peptides were immobilized on the chip in HBS-EP running buffer [10 mM HEPES (pH 7.4), 150 mM NaCl, 3 mM EDTA, 0.005% polysorbate 20 (v/v)]. The corresponding biotinylated P-peptides were diluted to between 10 pM and 1 μM in HBS-EP running buffer and injected at 2 μL/min until a suitable level of response was obtained (100−160 RU). The level of immobilized peptides was carefully determined to minimize mass transport limitations.

To measure the association of the Grb2 protein and the Grb2 SH2 domain with ErbB-derived P-peptides, a continuous flow of HBS-EP running buffer was maintained at 20 μL/min, and different concentrations of Grb2 proteins (1.95−500 nM) were passed over the immobilized peptides for 2 min. The dissociation constant was measured in free HBS-EP running buffer for 2 min. To remove the protein from the peptide, a regeneration buffer (10 mM glycine-HCl, pH 2.0 or 1.5, or 50 mM sodium hydroxide) was applied. The specific binding of protein−P-peptides were obtained by subtracting the nonspecific protein binding of the corresponding unphosphorylated peptides or blank chip. The data were analyzed using BIAevaluation 3.0 software to determine the association rate constant (k_{ass}) and the dissociation rate constant (k_{diss}) with a nonlinear least-squares method. K_D was obtained by calculating k_{diss}/k_{ass}. We performed three independent measurements for each protein−peptide interaction and obtained the average.

System Setup for MD Simulation. The X-ray structure of Grb2 SH2 domain, which is 98 amino acids long (a.a. 56−153) and bound with EpYIN (P-peptide; EGF receptor pY1068), was taken from the Protein Data Bank (pY; phosphotyrosine) (Figure 1) (*29*). The PDB entry was 1ZFP. The complex structures of P-peptides (Table 1) with Grb2 SH2 domain used in this study were constructed based on the X-ray structure using MOE (Chemical Computing Group, Inc.). The following modeling procedures were used: (1) amino acid residues were added, deleted, or replaced with

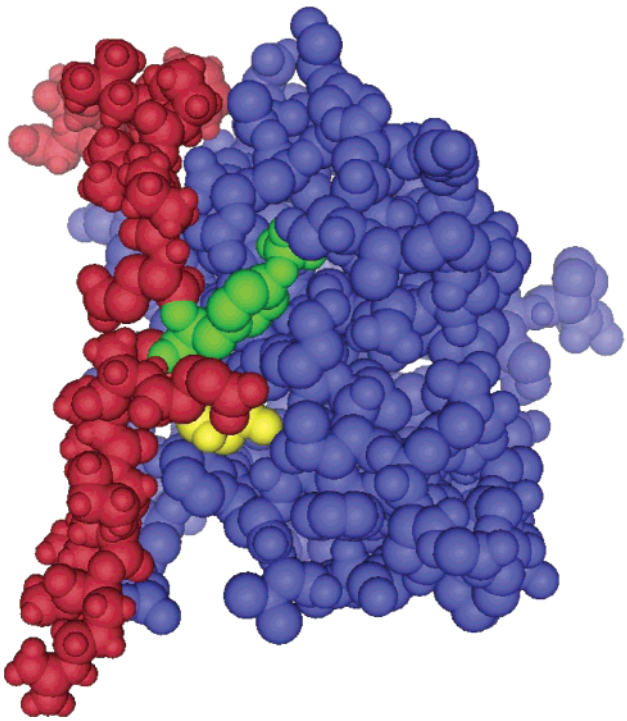

FIGURE 1: Crystal structure of the Grb2−P-peptide complex (pY1068, PDB 1ZFP). The structure is shown using a space filled model. The Grb2 is blue, and P-peptide is red. Phosphotyrosine and N at $p + 2$ are green and yellow, respectively.

appropriate residue manually and (2) the structure was energy minimized in a vacuum with all atom position fixing of the Grb2 SH2 domain. The Grb2 SH2 domain was extracted from the Grb2−pY1068 complex as the initial structure for MD simulation of free Grb2. Nine P-peptides were also extracted from each complexed structure as the initial structures for MD simulations of the free P-peptides. Partial phosphotyrosine charges, which are not included in the standard parm96 parameter set (*30*), were calculated using RHF/6−31*G single point calculation with Gaussian98 (Gaussian, Inc.) and the restrained electrostatic potential (RESP) method (*31*). The N and C termini of the P-peptides were capped by acetyl and *N*-methyl groups, respectively. The nine modeling complexes, free Grb2, and nine free P-peptides were surrounded by TIP3P water molecules (*32*) spherically. The size of each sphere was chosen so that the distance of the atoms in the protein from the wall was greater than 15.0 Å. The fully solvated systems were minimized using 100 steps of steepest descent followed by 4900 steps of conjugate gradient method.

Equilibration and MD Simulation. All MD simulations were carried out using the modified Amber 6.0 (*33*) for MDM on a PC (Athlon 1.6 GHz) with an MD-Grape2 board (2 chips; 64 Gflops) (*28*). The parm96 force field (*30*) was adopted, and time step was set at 1 fsec. All nonbonded interactions, van der Waals, and Coulomb forces and energies were calculated using MDM. The bond lengths involving hydrogen atoms were constrained to equilibrium lengths using the SHAKE method (*34*). The temperature of each system was gradually heated to 300 K during the first 100 ps period, and additional 900 ps MD simulations were performed for data collection. The temperature was kept constant at 300 K using the method of Berendsen et al. (*35*) coupled to a temperature bath with coupling constants of 0.2 ps.

Table 2: Grb2−P-Peptide Binding Affinity

P-peptide	binding protein	k_a ($\times 10^4$ M^{-1} s^{-1})	k_d ($\times 10^{-3}$ s^{-1})	K_D (nM)
pY1086	Grb2 full	0.464 ± 0.046	0.891 ± 0.020	192.0 ± 23.0
	Grb2 SH2	84.2 ± 4.2	7.32 ± 0.17	8.69 ± 0.63
pY1188	Grb2 full	10.1 ± 4.6	7.56 ± 0.40	74.5 ± 37.5
	Grb2 SH2	3.46 ± 0.49	2.54 ± 0.13	73.3 ± 14.1
pY1068	Grb2 full	1.09 ± 0.13	0.608 ± 0.063	56.0 ± 12.3
	Grb2 SH2	81.8 ± 1.9	3.30 ± 0.06	4.03 ± 0.17
pY1242	Grb2 full	5.34 ± 0.20	9.53 ± 0.10	178.0 ± 9.0
	Grb2 SH2	3.15 ± 0.16	2.99 ± 0.18	94.7 ± 10.4
pY1148	Grb2 full	W[a]	W	W
	Grb2 SH2	13.8 ± 0.6	4.03 ± 0.16	29.2 ± 2.5
pY1056	Grb2 full	NB[b]	NB	NB
	Grb2 SH2	NB	NB	NB
pY1173	Grb2 full	NB	NB	NB
	Grb2 SH2	NB	NB	NB
pY1045	Grb2 full	NB	NB	NB
	Grb2 SH2	NB	NB	NB
pY0992	Grb2 full	NB	NB	NB
	Grb2 SH2	NB	NB	NB

[a] Weak binding. [b] No binding.

MM-PBSA. The binding free energy is calculated as

$$\Delta G_{\text{binding}} = G(\text{complex}) - [G(\text{free Grb2}) + G(\text{free P-peptide})] \quad (1)$$

$$G(\text{molecule}) = \langle E_{\text{MM}} \rangle + \langle G_{\text{solvation}}^{\text{polar}} \rangle + \langle G_{\text{solvation}}^{\text{nonpolar}} \rangle - TS \quad (2)$$

$$\langle E_{\text{MM}} \rangle = \langle E_{\text{internal}} \rangle + \langle E_{\text{electrostatic}} \rangle + \langle E_{\text{vdW}} \rangle \quad (3)$$

$$G_{\text{solvation}}^{\text{nonpolar}} = \gamma A + b \quad (4)$$

The production MD trajectory was collected for a 300 ps period (from 700 to 1000 ps) with each snapshot saved every 10 ps. The set of structures obtained by an MD trajectory was sampled for use in estimating binding free energies. In the analysis of the binding free energies, the water molecules were replaced with implicit solvation models. < > denotes the average for a set of structures along an MD trajectory. E_{internal} includes the bond, angle, and torsional angle energies, and $E_{\text{electrostatic}}$ and E_{vdW} are intermolecular electrostatic and vdW energies, respectively. The $G_{\text{solvation}}^{\text{polar}}$ was calculated by solving the PB equation using the MEAD program (*18*, *19*). PARSE (*36*), vdW radii, and parm96 charges were used in this calculation. The grid spacing used was 0.5 Å. The dielectric constants inside and outside the molecule were 4.0 and 80.0, respectively. In eq 4, which calculates the nonpolar solvation contribution, A is the solvent accessible surface area calculated using the MSMS program (*20*), and γ and b are 0.00542 kcal/mol Å^2 and 0.92 kcal/mol, respectively. The probe radius was 1.4 Å. Normal-mode analysis was used to estimate conformational entropy, $-T\Delta S$, using the NMODE module in the Amber 6.0 software package.

RESULTS

SPR Analysis. Overall, full-length Grb2 protein and Grb2 SH2 domain showed the same specificity for the all ErbB-derived P-peptides in the SPR analysis (Table 2). However,

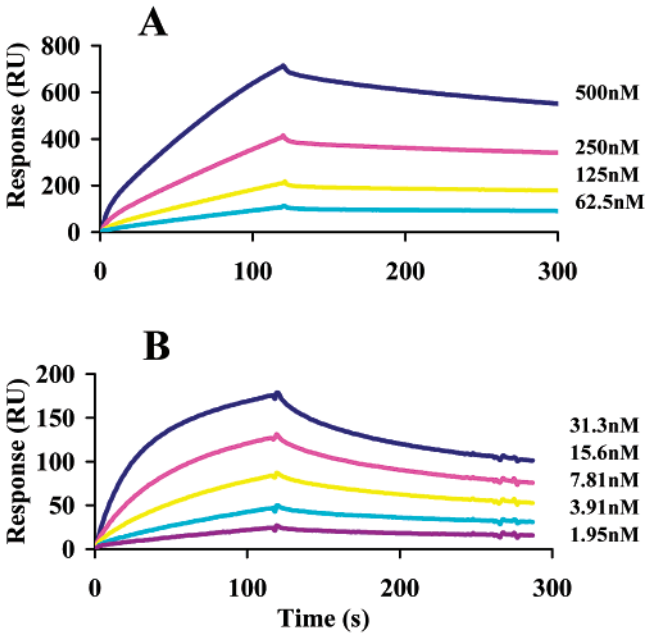

FIGURE 2: Binding of Grb2 to immobilized ErbB1 pY1068 phosphopeptide. (A) Sensorgrams for the binding of full-length Grb2 protein, with concentration of Grb2 in the range of 62.5−500 nM. (B) Sensorgrams for Grb2 SH2 domain, with concentration of the protein in the range of 1.95−31.3 nM.

the SH2 domain showed relatively higher affinity (smaller K_D) than the full-length Grb2 protein for all P-peptides. The sensorgrams of the interaction pattern between the Grb2 protein/Grb2 SH2 domain and the pY1068 peptide were virtually identical (Figure 2).

In this study, ErbB1-derived pY1068, pY1086, pY1148 and ErbB4-derived pY1188 and pY1242 were identified as specific Grb2 binding peptides. With the exception of pY1148, all of these peptides possessed the pYXNX motif. The results for pYXNX peptides were consistent with those of previous sequence study (*12*). Although ErbB4-derived pY1188 and pY1242 were identified as the Shc binding sites in cellular experiments (*13*), our study found that these sites may also work for Grb2 binding. The results for pY1068 and pY1086 were qualitatively consistent with a previous study involving SPR analysis using Grb2 GST fusion proteins where their affinities were 30 and 60 nM, respectively (*9*). We also tested an effect of different flow rates (20, 30, 40, and 50 μL/min) on the interaction analysis. Our results essentially showed identical binding curves and K_D; therefore, we concluded that there was no effect of the flow rates on the data obtained.

MD Simulations. We performed 1 ns MD simulations of nine Grb2−P-peptides complexes (Table 1), a free Grb2, and nine free P-peptides (Table 1) to estimate their binding free energies (19 ns total). The backbone heavy atom root-mean-square (rms) deviations of the Grb2 and the P-peptides from the initial modeling structure for each simulation are shown in Figure 3. In Grb2−P-peptide complex simulations, Grb2 was very stable with the rms deviation <1.5 Å (Figure 3A). We also performed an MD simulation of free Grb2 to calculate G (free Grb2) in eq 1, and this rms deviation was also small (<1.5 Å, Figure 3C). Since the initial structures of all P-peptides in our MD simulations were modeled, the rms deviations of the P-peptides (complexed and free) fluctuated greatly (Figure 3B,D).

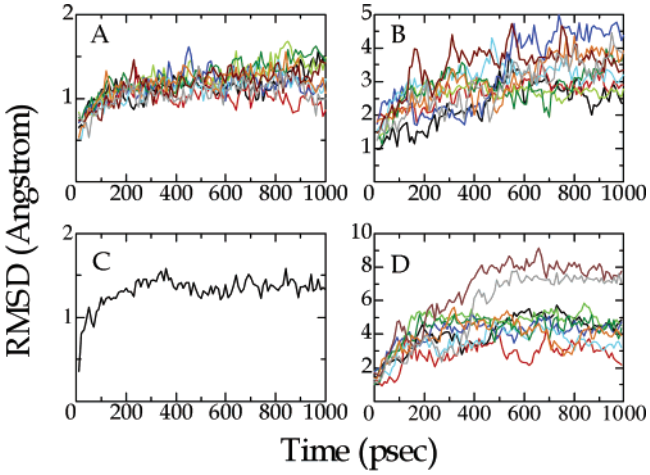

FIGURE 3: Backbone heavy atom rms deviations of the Grb2 (A), complexed P-peptides (B), free Grb2 (C), and free P-peptides (D) from initial modeling structures as a function of simulation time. Black line, pY0992; red line, pY1068; light green line, pY1086; blue line, pY1045; cyan line, pY1148; dark green line, pY1173; orange line, pY1056; brown line, pY1242; and gray line, pY1188.

Binding Free Energies of Grb2−P-Peptides. In our experiments, the only exception to the pYXNX rule was the ErbB1 pY1148. The pY1148 peptide showed either weak or strong affinity for Grb2 protein or its SH2 domain, whereas the other P-peptides (pY0992, pY1045, pY1056, and pY1173) showed no affinity for the Grb2 (Table 2). The calculated and measured binding free energies of the set of P-peptides to Grb2 SH2 domain are shown in Table 3. The binding free energies obtained with MM-PBSA were in excellent qualitative agreement with our SPR analysis. The correlation coefficient between calculated and experimental binding free energies was 0.92 (Figure 4). The P-peptides with a consensus sequence of pYXNX (pY1068, pY1086, pY1188, and pY1242) showed favorable binding affinity for the Grb2 (Tables 2 and 3), consistent with previous experimental studies (*8*−*11*). An unexpected observation was that a P-peptide with pYQQD (pY1148), which had not been identified as a direct binding site of the Grb2 in earlier studies, also showed favorable binding affinity for the Grb2 in our experimental and computational analyses (Tables 2 and 3).

Component Analysis of Binding Free Energies. The correlation coefficients between the measured binding free energies and each component of the calculated figures were compared to identify what energetic factors were dominant for binding affinity (Table 4). We found that van der Waals energy (vdW term, r was 0.69) and nonpolar solvation contribution (SA term, r was 0.73) had better correlation with binding affinity. The other components—the electrostatic interaction energy (Coulomb term, r was 0.45), the electrostatic solvation energy (PB term, r was 0.47), and the entropy contribution (r was 0.01)—showed no correlation (Table 4). The SA term was smaller than the vdW term in the order of 10 (Table 3). Therefore, we considered the van der Waals interactions between the Grb2 and the P-peptide to be the dominant factor for binding affinity. To clarify this, we analyzed the Grb2−P-peptide interfaces. During 1 ns MD simulations, phosphotyrosine formed hydrogen bonds stably with R31 and S33 in Grb2 (Figure 5), irrespective of its binding affinities. In the cases of specific binding of

Table 3: Component Analysis of Calculated Binding Free Energies

P-peptides	ΔE_{vdW}[a]	ΔE_{ele}	ΔG_{PB}	ΔG_{ele}[b]	ΔG_{SA}	$-T\Delta S$	ΔG_{calc}[c]	ΔG_{exp}[d]
pY1068	−74.69	−178.36	337.38	159.02	−6.56	34.09	45.42	−11.44
pY1086	−97.41	−129.87	341.67	211.80	−8.41	33.25	57.90	−10.99
pY1148	−56.41	−159.17	369.39	210.22	−4.27	29.60	61.81	−10.27
pY1188	−46.24	−55.37	258.07	202.70	−4.04	34.91	69.29	−9.73
pY1242	−46.24	−124.82	272.45	147.63	−3.17	32.65	77.91	−9.57
pY1173	−66.07	−222.42	340.36	117.94	−5.16	32.67	80.46	NB
pY1045	−50.04	−192.43	304.14	111.71	−4.47	32.24	80.49	NB
pY1056	−20.80	−126.12	235.59	109.47	−4.89	30.55	86.08	NB
pY0992	−62.79	−191.28	504.96	313.68	−5.29	32.40	198.47	NB

[a] All energies are in kcal/mol. [b] ΔG_{ele} is $\Delta E_{ele} + \Delta G_{PB}$. [c] Averaged standard deviation of calculated binding free energy is 4.98 kcal/mol. [d] Averaged standard deviation of measured binding free energy is 0.06 kcal/mol. NB indicates no binding.

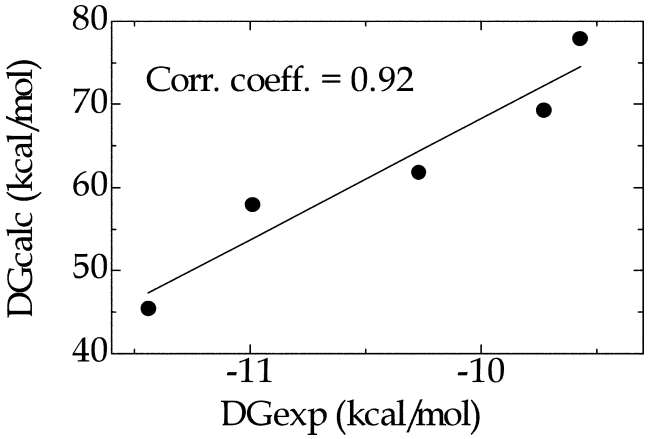

FIGURE 4: Correlation between calculated and experimental binding free energy.

Table 4: Correlation Coefficients between Components of Calculated Binding Free Energies and Measured Binding Free Energies

energy term	ΔE_{vdW}	ΔE_{ele}	ΔG_{PB}	ΔG_{ele}[a]	ΔG_{SA}	$-T\Delta S$
r	0.69	0.45	0.47	0.02	0.73	0.01

[a] $\Delta G_{ele} = \Delta E_{ele} + \Delta G_{PB}$.

P-peptides to the Grb2, such as with pY1068, pY1086, pY1188, and pY1242, there was an N at $p + 2$ (*pYXNX*). The N at $p + 2$ also formed hydrogen bonds stably with K54 and L65 during the MD simulations (Figure 5). In contrast, in the cases of unbound P-peptides (such as pY0992), we could find no hydrogen bonds around phosphotyrosine, and the distance between the Grb2 and the P-peptide became large (Figure 5). Interestingly, in the cases of pY1148 and pY1045, which have Q and S at $p + 2$, the Q and S formed hydrogen bonds with K54 and L65 in the same way as specific binding P-peptides. However, the distances between Grb2 and P-peptide were larger in pY1148 and smaller in pY1045 than those of specific binding P-peptides (Figure 5) derived from long side chains. The unexpected binding of the pY1148 to Grb2 may have been caused by the formation of the hydrogen bonds between Q at $p + 2$ and Grb2 at favorable distances between the two molecules. In contrast, pY1045 no longer showed specific binding (Tables 2 and 3) caused by the clash of the P-peptide with the Grb2, even though S at $p + 2$ formed hydrogen bonds with K54/L65 (Figure 5). From these results, we concluded that not only the formation of hydrogen bonds at $p + 2$ (Coulomb interaction) but also the van der Waals packing between the Grb2 and P-peptide is a key interaction for their specific binding. Thus, our speculation that van der Waals interactions between the Grb2 and the P-peptide are the dominant factor for binding affinity is reasonable.

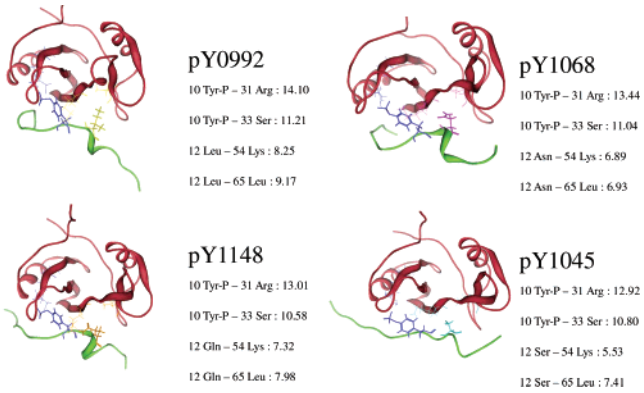

FIGURE 5: Hydrogen bonding patterns between Grb2 and P-peptides. Grb2 and P-peptide are represented by ribbons and colored red and green, respectively. Phosphotyrosine is represented by sticks and colored blue. L12, N12, Q12, and S12 at $p + 2$ are represented by sticks and colored in yellow, purple, orange, and cyan, respectively. R31, S33, K54, and L65 are represented by wireframe and colored the same as their corresponding binding residues, phosphotyrosine or $p + 2$. Cα−Cα distances between amino acids are in Å.

DISCUSSION

Amplification and mutation of ErbB receptors are implicated in the incidence of certain types of human cancers and has been regarded as the primary target for antitumor agent screening (*37*, *38*). The ErbB receptors are tyrosine phosphorylated after the binding of growth factors and recruit several kinds of signaling cassettes, causing distinct cellular responses such as cellular proliferation and differentiation. Grb2 is an adaptor protein that mediates the interaction of phosphorylated-ErbB receptor with Sos protein and plays an important role in regulating the signal transduction cascade. In this study, we compared the binding affinity of Grb2 and P-peptides derived from ErbB1 and ErbB4 receptors.

Of all the P-peptides (ErbB1-derived pY0992, pY1045, pY1068, pY1086, pY1148, and pY1173 and ErbB4-derived pY1056, pY1188, and pY1242), pY1068, pY1086, pY1188, and pY1242 showed clear specific binding to Grb2 protein in the experimental measurements and calculations, and these results were consistent with earlier results obtained with SPR and cellular experiments (*9*−*11*). However, our assay showed that pY1148 was also a specific ligand for full-length and SH2 domain of Grb2 protein. In an earlier study, pY1148

was shown to bind to the ErbB1 receptor mutant retaining pY1148 in cellular co-immunoprecipitation assay; however, a peptide inhibition study showed that pY1148 did not act as a direct Grb2 binding site; therefore, it had been thought that Grb2 bound with pY1148 through another adaptor protein (*11*, *39*). However, our MD simulations and free energy analysis results also reproduced this specific binding. Considering the fact that pY0992, pY1045, pY1056, and pY1173 peptides showed no affinity for Grb2 SH2 domain, the binding of pY1148 to this protein seems to be rather specific.

The calculated binding free energies were larger than those obtained by experiment. This result may have been caused by the short time scale of the MD simulations. However, the calculated free energies were qualitatively highly consistent with the experimental results, with a correlation coefficient of 0.92. For quantitative analysis, we need to perform longer MD simulations, especially for complexes and free P-peptides. These simulations should probably be performed for 10 ns or more for equilibration of the P-peptide as the P-peptides are short (14−21 amino acids long) and all of the initial structures for these P-peptides were similar to the extended structure. We are planning to perform these longer MD simulations using Protein Explorer, which is special purpose computer for MD and will be faster than MDM and developing in our team.

The dominant factor for the binding affinity was van der Waals interactions between Grb2 and P-peptide from component analysis of the calculated binding free energies. From this analysis, we concluded that the unexpected binding affinity of the pY1148 was caused by cooperation between Coulomb and van der Waals interactions (i.e., formation of hydrogen bonds between Q at $p + 2$ and K54/L65) and maintenance of an appropriate distance between the P-peptide and the Grb2. Therefore, the MD simulation in this study well-reflected the cellular phenomena, regardless of possession of the consensus sequence, pYXNX.

ACKNOWLEDGMENT

We wish to thank Ms. Mihoro Saeki and Ms. Ryoko Ushikoshi for the construction of the Grb2 expression vector and the expression and purification of the Grb2 protein. We would also like to thank Dr. Yoshinori Hirano for his help in using Gaussian98.

REFERENCES

1. Nioche, P., Liu, W. Q., Broutin, I., Charbonnier, F., Latreille, M. T., Vidal, M., Roques, B., Garbay, C., and Ducruix, A. (2002) *J. Mol. Biol. 315*, 1167−117.
2. Lowenstein, E. J., Daly, R. J., Batzer, A. G., Li, W., Margolis, B., Lammers, R., Ullrich, A., Skolnik, E. Y., Bar-Sagi, D., and Schlessinger, J. (1992) *Cell 70*, 431−442.
3. Pawson, T., and Nash, P. (2000) *Genes Dev. 14*, 1027−1047.
4. Cussac, D., Frech, M., and Chardin, P. (1994) *EMBO J. 13*, 4011−4021.
5. MacDonald, J. I., Gryz, E. A., Kubu, C. J., Verdi, J. M., and Meakin, S. O. (2000) *J. Biol. Chem. 275*, 18225−18233.
6. Alroy, I., and Yarden, Y. (1997) *FEBS Lett. 410*, 83−86.
7. Benjamin, C. W., Linseman, D. A., and Jones, D. A. (1994) *J. Biol. Chem. 269*, 31346−31349.
8. Ladbury, J. E., Lemmon, M. A., Zhou, M., Green, J., Botfield, M. C., and Schlessinger, J. (1995) *Proc. Natl. Acad. Sci. U.S.A. 92*, 3199−3203.
9. Batzer, A. G., Rotin, D., Urena, J. M., Skolnik, E. Y., and Schlessinger, J. (1994) *Mol. Cell Biol. 14*, 5192−5201.
10. Chook, Y. M., Gish, G. D., Kay, C. M., Pai, E. F., and Pawson, T. (1996) *J. Biol. Chem. 271*, 30472−30478.
11. Okutani, T., Okabayashi, Y., Kido, Y., Sugimoto, Y., Sakaguchi, K., Matuoka, K., Takenawa, T., and Kasuga, M. (1994) *J. Biol. Chem. 269*, 31310−31314.
12. Kessels, H. W., Ward, A. C., and Schumacher, T. N. (2002) *Proc. Natl. Acad. Sci. U.S.A. 99*, 8524−8529.
13. Cohen, B. D., Green, J. M., Foy, L., and Fell, H. P. (1996) *J. Biol. Chem. 271*, 4813−4818.
14. Srinivasan, J., Cheatham, T. E., III, Cieplak, P., Kollman, P. A., and Case, D. A. (1998) *J. Am. Chem. Soc. 120*, 9401−9409.
15. Kollman, P. A., Massova, I., Reyes, C., Kuhn, B., Huo, S., Chong, L., Lee, M., Lee, T., Duan, Y., Wang, W., Donini, O., Cieplak, P., Srinivasan, J., Case, D. A., and Cheatham, T. E., III. (2000) *Acc. Chem. Res. 33*, 889−897.
16. Gilson, M. K., and Hoing, B. (1988) *Proteins 4*, 7−18.
17. Hoing, B., and Nicholls, A. (1995) *Science 268*, 1144−1149.
18. Bashford, D., and Gerwert, K. (1992) *J. Mol. Biol. 224*, 473−486.
19. Bashford, D. (1997) in *Scientific Computing in Object-Oriented Parallel Environments*. (Ishikawa, Y., Oldehoeft, R. R., Reynders, J. V. W., and Tholburn, M., Eds.) pp 233−240, 1343, ISCOPE97, Springer, Berlin.
20. Sanner, M. F., Olson, A. J., and Spehner, J. C. (1996) *Biopolymers 38*, 305−320.
21. Massova, I., and Kollman, P. A. (1999) *J. Am. Chem. Soc. 121*, 8133−8143.
22. Brooks, B. R., Janežič, D., and Karplus, M. (1995) *J. Comput. Chem. 16*, 1522−1553.
23. Chong, L. T., Duan, Y., Wang, L., Massova, I., and Kollman, P. A. (1999) *Proc. Natl. Acad. Sci. U.S.A. 96*, 14330−14335.
24. Kuhn, B., and Kollman, P. A. (2000) *J. Med. Chem. 43*, 3786−3791.
25. Wang, J., Morin, P., Wang, W., and Kollman, P. A. (2001) *J. Am. Chem. Soc. 123*, 5221−5230.
26. Wang, W., Lim, W. A., Jakalian, A., Wang, J., Wang, J., Luo, R., Bayly, C. I., and Kollman, P. A. (2001) *J. Am. Chem. Soc. 123*, 3986−3994.
27. Huo, S., Wang, J., Cieplak, P., Kollman, P. A., and Kuntz, I. D. (2002) *J. Med. Chem. 45*, 1412−1419.
28. Narumi, T., Susukita, R., Ebisuzaki, T., McNiven, G., and Elmergreen, B. (1999) *Mol. Simul. 21*, 401−415.
29. Rahuel, J., Carcia-Echeverria, C., Furet, P., Strauss, A., Caravatti, G., Fretz, H., Schoepfer, J., and Gay, B. (1998) *J. Mol. Biol. 279*, 1013−1022.
30. Kollman, P. A., Dixon, R., Cornell, W., Fox, T., Chipot, C., and Pohorille, A. (1997) in *Computer simulations of biological systems* (van Gunsteren W. F., Ed.).
31. Bayly, C. I., Cieplak, P., Cornell, W. D., and Kollman, P. A. (1993) *J. Phys. Chem. 97*, 10269−10280.
32. Jorgensen, W. L., Chandrasekhar, J., Madura, J. D., Impey, R. W., and Klein, M. L. (1983) *J. Chem. Phys. 79*, 926−935.
33. Case, D. A., Pearlman, D. A., Caldwell, J. W., Cheatham, T. E., III, Ross, W. S., Simmerling, C., Darden, T., Merz, K. M., Stanton, R. V., Cheng, A., Vincent, J. J., Crowley, M., Tsui, V., Radmer, R., Duan, Y., Pitera, J., Massova, I., Seibel, G. L., Singh, U. C., Weiner, P., and Kollman, P. A. (1999) *Amber 6.0*, University of California, San Francisco.
34. Ryckeart, J.-P., Ciccotti, G., and Berendsen, H. J. C. (1977) *J. Comput. Chem. 23*, 327−341.
35. Berendsen, H. J. C., Postma, J. M. P., van Gunsteren, W. F., DiNola, A., and Haak, J. R. (1984) *J. Comput. Phys. 81*, 3684−3690.
36. Sitkoff, D., Sharp, K. A., and Honig, B. (1994) *J. Phys. Chem. 98*, 1978−1988.
37. Blume-Jensen, P., and Hunter, T. (2001) *Nature 411*, 355−365.
38. Yarden, Y., and Sliwkowski, M. X. (2001) *Nat. Rev. Mol. Cell Biol. 2*, 127−137.
39. Okabayashi, Y., Kido, Y., Okutani, T., Sugimoto, Y., Sakaguchi, K., and Kasuga, M. (1994) *J. Biol. Chem. 269*, 18674−18678.

BI034113H